

# TCR signal initiation machinery is pre-assembled and activated in a subset of membrane rafts

Philippe Drevot, Claire Langlet, Xiao-Jun Guo<sup>1</sup>, Anne-Marie Bernard, Odile Colard<sup>2</sup>, Jean-Paul Chauvin<sup>3</sup>, Rémi Lasserre and Hai-Tao He<sup>4</sup>

Centre d'Immunologie de Marseille-Luminy, CNRS-INSERM-Université de la Méditerranée, Case 906, F-13288 Marseille Cedex 9, <sup>1</sup>LBBN, CNRS-ESA 6033, Faculté des Sciences et Techniques de Saint-Jérôme, F-13397 Marseille Cedex 20, <sup>2</sup>INSERM U538, CHU Saint-Antoine, 27 rue de Chaligny, F-75012 Paris and <sup>3</sup>LGPD-IBDM, Case 907, F-13288 Marseille Cedex 9, France

<sup>4</sup>Corresponding author  
e-mail: he@ciml.univ-mrs.fr

P.Drevot and C.Langlet contributed equally to this work

**Recent studies suggest that rafts are involved in numerous cell functions, including membrane traffic and signaling. Here we demonstrate, using a polyoxyethylene ether Brij 98, that detergent-insoluble microdomains possessing the expected biochemical characteristics of rafts are present in the cell membrane at 37°C. After extraction, these microdomains are visualized as membrane vesicles with a mean diameter of ~70 nm. These findings provide further evidence for the existence of rafts under physiological conditions and are the basis of a new isolation method allowing more accurate analyses of raft structure. We found that main components of T cell receptor (TCR) signal initiation machinery, i.e. TCR-CD3 complex, Lck and ZAP-70 kinases, and CD4 co-receptor are constitutively partitioned into a subset of rafts. Functional studies in both intact cells and isolated rafts showed that upon ligation, TCR initiates the signaling in this specialized raft subset. Our data thus strongly indicate an important role of rafts in organizing TCR early signaling pathways within small membrane microdomains, both prior to and following receptor engagement, for efficient TCR signal initiation upon stimulation.**

**Keywords:** lipid raft/membrane domain/signal transduction/T cell receptor

## Introduction

Membrane rafts are found in all mammalian cell types as well as in *Drosophila*, *Dictyostelium* and yeast (Simons and Ikonen, 1997; Brown and London, 1998; Simons and Toomre, 2000). Not only are rafts enriched in sphingolipids (sphingomyelins and glycosphingolipids) and cholesterol, but these constituents are essential for the formation of rafts (Simons and Ikonen, 1997; Brown and London, 2000). An increasing amount of data suggest that rafts play fundamental roles in diverse cellular functions, particularly in signal transduction, by promoting a

segregated arrangement of membrane proteins and lipids (Brown and London, 2000; Simons and Toomre, 2000).

Studies in model membranes indicate that rafts correspond to a phase of the lipid bilayer, namely the liquid-ordered (lo) phase (Brown and London, 2000; Simons and Toomre, 2000). The formation of this lo phase is promoted by sphingolipids, the long saturated acyl chains of which allow tight molecular packing (Brown and London, 2000), and further facilitated by the presence of cholesterol (Simons and Ikonen, 1997; Brown and London, 2000). The use of GPI-anchored proteins and other raft markers to investigate the existence of rafts in living cells has revealed that they are usually very small in size (Simons and Toomre, 2000).

Engagement of the T cell receptor (TCR) by its specific peptide-MHC (pMHC) ligand triggers intracellular signaling cascades that are required for T lymphocyte development and functions (for a review see Weiss and Littman, 1994). Such cascades are initiated by the activation of a signal transduction machinery, the main components of which include the TCR $\alpha\beta$  heterodimer and the tightly associated CD3  $\epsilon$ ,  $\gamma$ ,  $\delta$  and  $\zeta$  polypeptides, Lck and ZAP-70 kinases, and the CD4 (or CD8) co-receptor. Recognition of pMHC by TCR results in phosphorylation of the cytoplasmic domains of the CD3 complex by the *src* kinase Lck, which permits the recruitment and activation of the *syk* kinase ZAP-70 (Weiss and Littman, 1994). During pMHC recognition, CD4 (also CD8) is believed to bind to the same pMHC molecule as the TCR, thus contributing to the recruitment of the Lck via its cytoplasmic tail to the TCR-CD3 complex engaged by the class II (I) pMHC (Janeway, 1992). This tyrosine kinase recruitment strongly 'boosts' TCR recognition (Janeway, 1992; Krummel *et al.*, 2000).

Recent reports have ascribed a crucial role for rafts in the activation of the TCR signaling cascades (Montixi *et al.*, 1998; Moran and Miceli, 1998; Xavier *et al.*, 1998; Zhang *et al.*, 1998; Janes *et al.*, 1999; for reviews see Langlet *et al.*, 2000; Harder, 2001). In particular, upon TCR engagement the activated TCR-CD3-ZAP-70 complexes are found within rafts where they phosphorylate the raft resident protein LAT (linker for the activation of T cells), the major substrate of ZAP-70 and a central signaling scaffold (for a review see Zhang and Samelson, 2000).

Although substantial evidence supports the implication of rafts in TCR-dependent signaling cascades, a key issue remains unclear: how is TCR ligation coupled to the activation events in rafts? Initial data (Montixi *et al.*, 1998; Xavier *et al.*, 1998) led to the proposition that TCR moves into rafts upon ligation, perhaps after an initial phosphorylation of the TCR-CD3 (Montixi *et al.*, 1998). ZAP-70 is then recruited to rafts by the phosphorylated TCR-CD3 and activated to phosphorylate LAT. However,

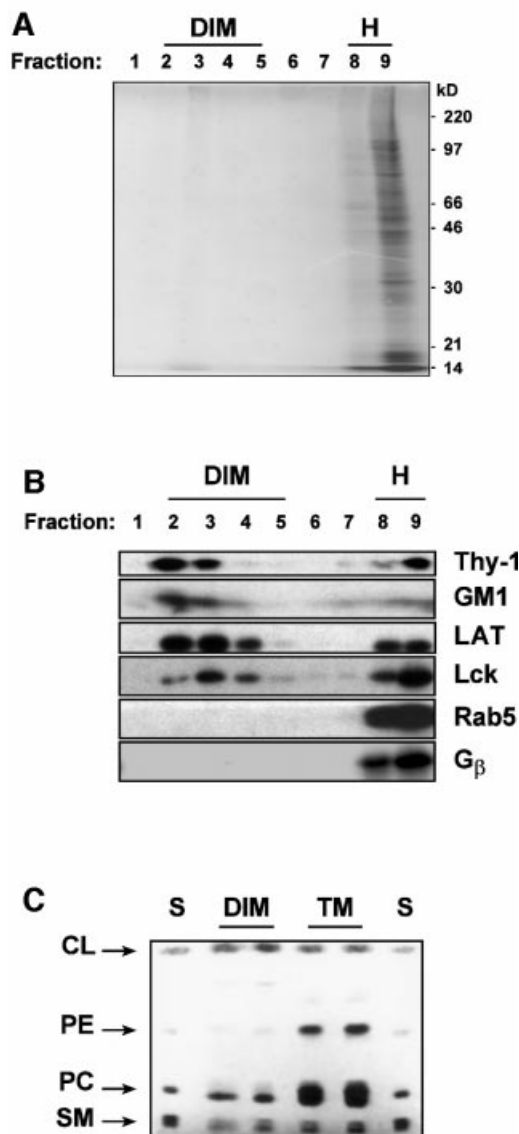


**Fig. 1.** (A) PNS of thymocytes ( $2 \times 10^8$ ) was treated with Brij 98 at  $37^\circ\text{C}$  and fractionated on a sucrose gradient as described in Materials and methods. A  $50 \mu\text{l}$  aliquot of each fraction was resolved on SDS-PAGE and stained with Coomassie Blue. The gel was scanned and protein bands were quantitated using the NIH image version 1.42 software system. (B) A  $50 \mu\text{l}$  aliquot of each fraction of the gradient was blotted with the specific probes, as indicated. For the analysis of  $\text{G}\beta$ , the PNS was treated with  $100 \text{ mM GTP}\gamma\text{S}$  in order to promote the dissociation between  $\text{G}\beta\gamma$  and  $\text{G}\alpha$ . (C) Lipids were extracted from thymocyte DIM fraction and from total membranes in the PNS and subjected to high-performance thin-layer chromatography (HPTLC) as described in the Supplementary data. Lipids extracted from DIMs (lanes DIM, each from  $9 \times 10^7$  cells) or from total membranes (lanes TM, each from  $3 \times 10^7$  cells) were revealed by primulin. Migration standards (lanes S) included: CL, cholesterol; PE, phosphatidylethanolamine; PC, phosphatidylcholine; SM, sphingomyelin.

some observations have suggested that the TCR-CD3 complex could already associate weakly with rafts prior to ligand binding (Montixi *et al.*, 1998; Janes *et al.*, 1999), which might be inefficiently detected by the cold Triton X-100-based raft isolation method (Janes *et al.*, 1999; Langlet *et al.*, 2000).

In this paper, we have demonstrated the existence of detergent-insoluble microdomains exhibiting the expected

biochemical characteristics of rafts at  $37^\circ\text{C}$ . These findings strongly support the existence of rafts at physiological temperature. They also are the basis for the development of a new raft-isolation method that has enabled us to investigate further the role of rafts in TCR signal transduction. We showed that a fraction of TCR-CD3 and ZAP-70 are constitutively associated to rafts. Moreover, using a  $\text{CD4}^+$  T cell line, we uncovered the existence a raft subset that localizes essentially all the raft-associated TCR-CD3 complex, enriched in the CD4 co-receptor and containing Lck and ZAP-70 kinases. Our results further indicated that TCR initiates signaling upon ligation in this raft subset, which is accompanied by rapid propagation to other raft populations. Taken together, these data provide new insights into how rafts take part in TCR signal transduction.

## Results

### *Isolation and characterization of detergent-insoluble membrane microdomains using Brij 98*

Lo and liquid-disordered (ld) phases display different behaviors when treated with non-ionic detergents. Resistance to solubilization by Triton X-100 at  $4^\circ\text{C}$  has been widely utilized as a basis for isolating raft membranes (Simons and Ikonen, 1997; Brown and London, 1998). However, Triton X-100-resistant membrane complexes could only be found at low temperatures. This raises the question of how well these membrane complexes reflect raft domains in cell membranes under physiological conditions, since chilling is believed to strongly modify the phase behavior of membranes (Brown and London, 2000). In addition, Triton X-100 has a limited capability to distinguish ordered from disordered membrane domains, since the lo phase is substantially solubilized by this detergent even at  $4^\circ\text{C}$  (Brown and London, 2000).

To find a detergent that could discriminate more ordered domains from their phospholipid environments at  $37^\circ\text{C}$  through selective solubilization of the latter, we screened members of the polyoxyethylene ether (Brij) series. We selected Brij 98, characterized by its relatively bulky polyoxyethylene headgroup and mono-unsaturated ether moieties, which predicted a preferential partitioning in (and therefore solubilization of) the loosely packed, fluid phase, rather than the tightly packed, ordered phase of the lipid bilayer.

Figure 1 shows that following incubation of a post-nuclear supernatant (PNS) of mouse thymocytes with 1% Brij 98 for 5 min at  $37^\circ\text{C}$ , low-density detergent-insoluble membranes (DIMs) are separated from the solubilized material by ultracentrifugation in a sucrose density gradient. The DIMs floated to the buoyant fractions, whereas the soluble counterpart remained in the heavy (H) fractions of the gradient. These DIMs contained only  $\sim 2.5\%$  of total proteins found in the PNS (Figure 1A), yet were markedly enriched in membrane proteins modified by saturated-chain lipids such as (GPI-anchored) Thy-1, (dual palmitoylated) LAT and (myristoylated and palmitoylated) Lck, as well as GM1 glycosphingolipid (Figure 1B). In contrast, membrane proteins modified by prenyl groups, which have a branched and bulky structure, such as Rab-5 and  $\text{G}\beta$  that

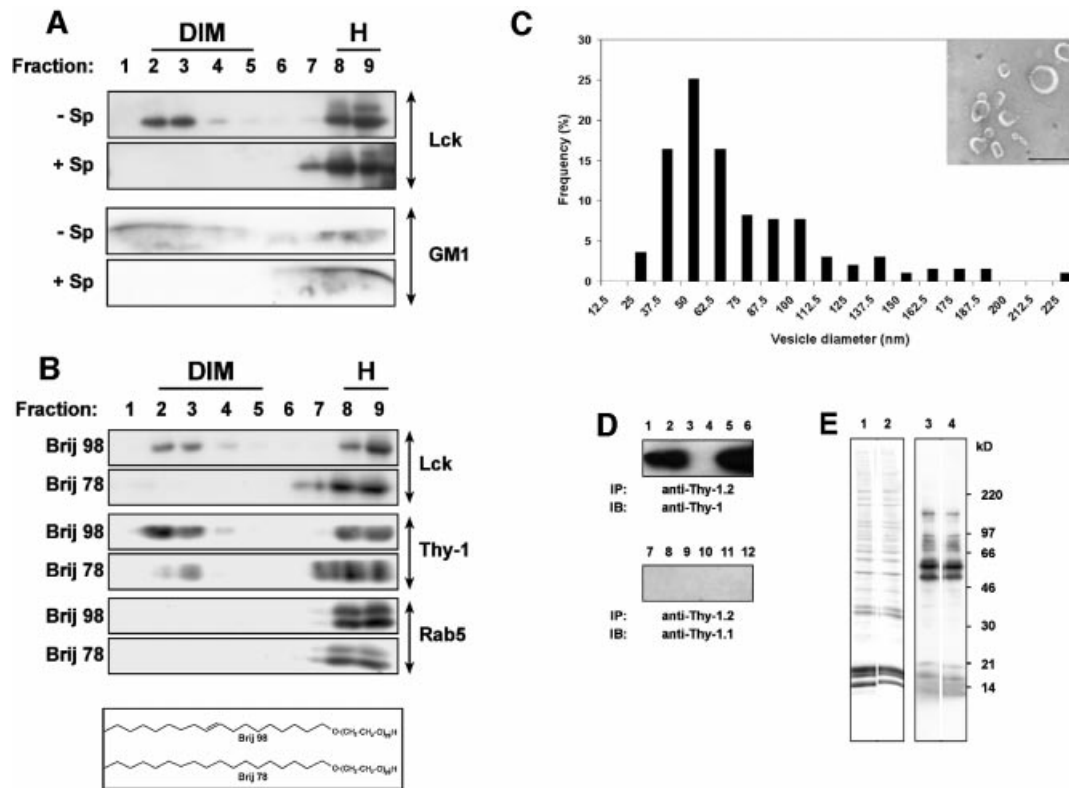


**Fig. 2.** (A) Thymocyte PNS was treated with Brij 98 at 37°C in the presence or absence of 0.2% saponin (Sp). The presence of DIMs was monitored by the distribution of Lck and GM1 over the sucrose gradient. (B) Thymocyte PNS was treated with Brij 98 or Brij 78 at 37°C, and fractionated in the sucrose density gradient before being blotted with the indicated antibodies (Abs). A schema of the structure of Brij 98 and Brij 78 is included. (C) Thymocyte DIMs were concentrated and subjected to EM analysis as described in the Supplementary data. DIM size was analyzed using Scion Image Beta 4.02 software and a representative result from a measurement of 195 vesicles is shown. Inset shows parts of an electron micrograph. Bar, 100 nm. (D) DIMs from Thy-1.2-expressing (lanes 1, 2, 7 and 8) or Thy-1.1-expressing (lanes 3, 4, 9 and 10) AKR1 thymomas, or a mixture (1:1) of both (lanes 5, 6, 11 and 12) were immunoprecipitated and blotted with the indicated mAbs. DIMs from  $3 \times 10^7$  (lanes 1, 3, 5, 7, 9 and 11) and  $6 \times 10^7$  (lanes 2, 4, 6, 8, 10 and 12) thymoma cells were analyzed. (E) Thymocyte PNS was either solubilized for 5 min with 1% Brij 98 at 37°C, diluted by the cold sucrose containing buffer A and boiling in SDS sample buffer (lanes 1 and 3), or immediately boiling in SDS sample buffer (lanes 2 and 4). The proteins were resolved on SDS-PAGE and revealed by Coomassie Blue staining (lanes 1 and 2) or immunoblotting with 4G10 anti-phosphotyrosine (PY) mAb (lanes 3 and 4).

should be partitioning to disordered phases (Melkonian *et al.*, 1999) were fully solubilized (Figure 1B).

Lipid analysis (Figure 1C) showed that, in comparison with the total membranes present in the PNS, DIMs were rich in sphingomyelins and cholesterol but poor in phospholipids. Indeed, quantitative studies indicated that the recovery of sphingomyelin, cholesterol and total phospholipids in DIMs were  $43 \pm 12.3\%$ ,  $32.9 \pm 3\%$  and  $9.4 \pm 2.2\%$ , respectively, of those found in total membranes. Therefore, both protein and lipid composition of DIMs correspond to those expected for raft domains (Simons and Ikonen, 1997; Brown and London, 2000).

Cholesterol is known to be critically involved in the formation of ordered raft domains (Simons and Ikonen, 1997; Brown and London, 2000). Therefore, we evaluated the effect of saponin on Brij 98 DIMs. Figure 2A indicates that cholesterol sequestration by saponin completely disrupts Brij 98 DIMs. Moreover, we observed a significant reduction of DIM recovery when Brij 78 ( $C_{18,0}E_{20}$ ) was used instead of Brij 98 ( $C_{18,1}E_{20}$ ) to solubilize membranes (Figure 2B). The two detergents have the same headgroup and only differ by one double bond present in the alkyl moiety of Brij 98, but not Brij 78. Although the two detergents display the same hydrophilic-lipophilic

balance (HLB = 15.3), Brij 78 is expected to have higher partitioning into the ordered domains and promotes their solubilization. Together, these results suggest that Brij 98 DIMs might exhibit properties of ordered domains. However, further investigation will be required to address this issue directly.

Electron microscopy examination shows that Brij 98 DIMs appear as membrane vesicles exhibiting a broad range of sizes with a mean diameter of  $67 \pm 39$  nm (Figure 2C). Fusion among heterologous membrane fragments did not take place during Brij 98 detergent extraction at 37°C, since from a mixture of cells expressing either Thy-1.1 or Thy-1.2 the isolated DIMs were positive for only one, but not both Thy-1 alleles (Figure 2D). These results also rule out *de novo* DIM formation *in vitro* during PNS chilling following detergent treatment at 37°C. Another concern related to the membrane solubilization at 37°C is the possible increase in enzymatic degradation. However, we found no significant difference in the profile of total and tyrosine phosphorylated (Ptyr) proteins in PNS subjected or not to the 37°C incubation step (Figure 2E). Besides the inclusion of enzymatic inhibitors, the relatively short solubilization period (5 min) seemed to be important in this context.

Our data thus suggest that Brij 98 DIMs correspond to the raft membrane microdomains that are present at physiological temperature.

### Constitutive partitioning and activation upon receptor ligation of TCR-CD3 and ZAP-70 in rafts

Using the new raft isolation procedure, we analyzed the initiation of TCR signaling pathways in these membrane domains. The first signaling events following TCR engagement include a series of protein tyrosine phosphorylations, particularly by Lck and ZAP-70 kinases. To examine these events, we used mature T lymphocytes rather than thymocytes, which display a marked heterogeneity in terms of cell populations and TCR responses. Figure 3A shows that a stimulation of 30 s with anti-CD3 $\epsilon$  monoclonal antibody (mAb) triggered an immediate appearance of P<sub>tyr</sub> substrates in both the raft and non-raft fractions. Nonetheless, each fraction displays a specific pattern. In the raft fraction, in addition to phospho-LAT, we also detected the phospho-CD3 $\zeta$  chain p23 $\zeta$  and phospho-ZAP-70. p23 $\zeta$  is fully phosphorylated at all of its three immunoreceptor tyrosine-based activation motifs (ITAMs) (van Oers *et al.*, 2000) and ZAP-70 phosphorylation indicates its catalytically active form (Weiss and Littman, 1994). Both events depend on Lck, and the appearance of p23 $\zeta$  has been correlated with the activation of ZAP-70 (van Oers *et al.*, 2000). The data in Figure 3A indicate that upon TCR stimulation the ratio of p23 $\zeta$  to either the constitutively phosphorylated p21 $\zeta$  or the non-phosphorylated np16 $\zeta$  were much higher in raft than non-raft compartments. This finding suggests that during TCR signal initiation the TCR-CD3 complex becomes highly activated in raft microdomains. Moreover, although a much stronger ZAP-70 signal was detected in the non-raft fraction, phospho-ZAP-70 was seen readily only in the raft fraction (also see Figure 3B). Taken together, these results strongly corroborate the suggestion that raft membrane microdomains play an important role in the activation of the earliest TCR signaling steps (Montixi *et al.*, 1998; Xavier *et al.*, 1998; Janes *et al.*, 1999).

In contrast to previous studies, we found that both the p21 $\zeta$  and np16 $\zeta$ , which account for the quasi-totality of the CD3 $\zeta$  chains, and ZAP-70 constitutively partitioned in rafts, and this distribution was not significantly modified following the TCR-CD3 engagement (Figure 3A). Semi-quantitative analysis using an anti-TCR mAb revealed that at steady state ~10% of the total TCR is associated with rafts in splenic T lymphocytes (Supplementary figure 1 available at *The EMBO Journal Online*).

We also conducted experiments in 3A9 T cell hybridomas harboring a TCR that recognizes a peptide (residues 48–63) of hen egg lysozyme (HEL) in the context of H-2A<sup>k</sup> (Liu *et al.*, 2000) to examine TCR signal transduction triggered directly by pMHC. To this end, 3A9 cells were incubated at 37°C for 30 s with LK35.2 antigen presenting cells prior to raft isolation. Supplementary figure 2 shows that addition of HEL peptide induced an immediate accumulation of P<sub>tyr</sub> proteins, including the phosphorylated forms of CD3 $\epsilon$ , CD3 $\zeta$ , ZAP-70 and LAT in rafts of 3A9 cells. In addition, we again observed a constitutive raft-partitioning of TCR-CD3 and ZAP-70. However, in contrast to primary T cells (Figure 3A), TCR

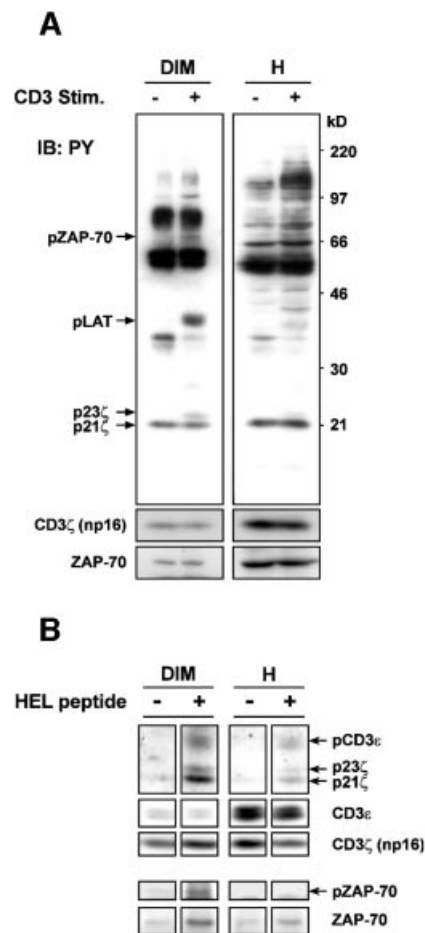


**Fig. 3.** (A) Nylon wool-purified splenic T cells ( $2 \times 10^8$ ) were stimulated or not with 15  $\mu\text{g/ml}$  of 145-2C11 anti-CD3 $\epsilon$  mAb at 37°C for 30 s. Proteins in raft (DIM) and one-quarter of non-raft (H) fractions were concentrated and blotted with anti-PY mAb. The positions of phospho-CD3 $\zeta$  p23 and p21, phospho-LAT and phospho-ZAP-70 are indicated. The blot was then stripped and reprobed with anti-CD3 $\zeta$  (that reveals non-phosphorylated CD3 $\zeta$  np16) and anti-ZAP-70 Abs, respectively. (B) 3A9 T cell hybridomas ( $2 \times 10^7$ ) were incubated for 30 s at 37°C with the paraformaldehyde-fixed LK35.2 B cells ( $1 \times 10^7$ ) pulsed with or without the HEL peptide, as described in Materials and methods. Raft (DIM) and non-raft (H) fractions were prepared and treated for raft solubilization with 60 mM *N*-octylglucoside for 1 h at 4°C, before being subjected to immunoprecipitation with 145-2C11 anti-CD3 $\epsilon$  mAb (Montixi *et al.*, 1998). Immunoprecipitates were blotted with anti-PY mAb. The blot was then stripped and reprobed with the indicated Abs.

stimulation in 3A9 cells resulted in an increase of ZAP-70 in rafts, which paralleled an augmentation of p21 $\zeta$ . Finally, the amount of TCR-CD3 in rafts remained unchanged following treatment with PP2, an inhibitor of *src* family kinases, indicating that the constitutive raft-association of TCR-CD3 occurs in a manner that is independent of *src* kinase activity (Supplementary figure 3).

Immunoprecipitation analysis shows that upon stimulation by the HEL peptide, TCR-CD3 complexes in the raft fraction are enriched in phospho-CD3 chains compared with the non-raft fraction (Figure 3B). It is of note that relative to the amount of CD3 $\epsilon$ , much less CD3 $\zeta$  was co-precipitated in the non-raft fraction. The reason for this is presently unknown. The most significant finding in

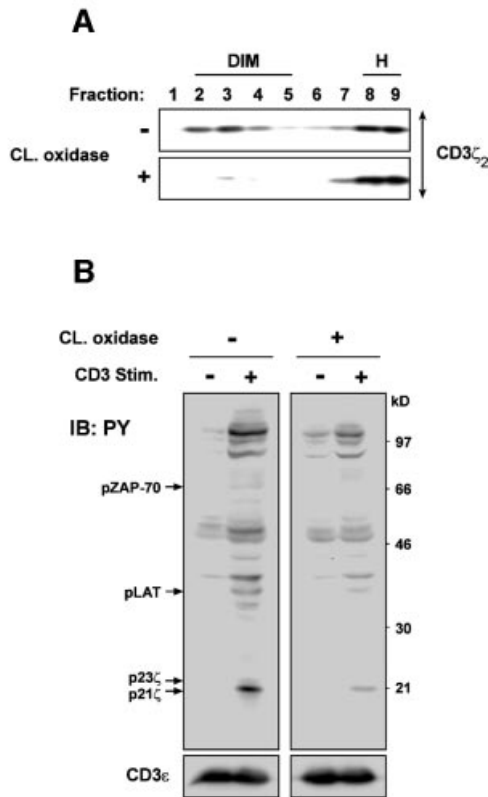


**Fig. 4.** (A) 3A9 cells ( $3 \times 10^7$ ) were treated, or not, with 4 U/ml of cholesterol oxidase at 37°C for 1 h. Brij 98 solubilized PNS was fractionated on the sucrose gradient and blotted with anti-CD3 $\zeta$  mAb. (B) 3A9 cells were treated or not with cholesterol oxidase as in (A). They were then stimulated with or without 15  $\mu$ g/ml of anti-CD3 $\epsilon$  mAb at 37°C for 30 s. The proteins in the total cell lysate were blotted with anti-PY mAb. The blot was then stripped and reprobed with anti-CD3 $\epsilon$  Ab.

this experiment was that although ZAP-70 could be co-immunoprecipitated from both raft and non-raft fractions by anti-CD3 $\epsilon$  mAb after TCR stimulation, phosphorylated (activated) ZAP-70 was only seen in the immunoprecipitate from the raft fraction (Figure 3B). Thus, these results demonstrate that raft microdomains are privileged membrane sites where TCR signaling initiation pathways are organized and activated.

#### **Rafts are required for the initiation of TCR signal transduction**

The requirement for rafts in early TCR signaling events such as induction of tyrosine phosphorylation and Ca<sup>2+</sup> flux has previously been studied by using methyl- $\beta$ -cyclodextrin as well as filipin and nystatin (Xavier *et al.*, 1998), all of which affect raft integrity via cholesterol depletion or sequestration (Simons and Toomre, 2000). However, some concerns have recently been raised about the use of these compounds as they seem to induce on their own transient tyrosine phosphorylation of the TCR signaling proteins, e.g. CD3 $\zeta$ , ZAP-70 and LAT in Jurkat T cells (Kabouridis *et al.*, 2000). To clearly establish the role of rafts in TCR signal transduction, we altered raft microdomains through membrane cholesterol modification by cholesterol oxidase. Xu and London

(2000) have recently reported that cholesterol, once oxidized, is incapable of promoting the formation of lo phases in model membranes. Moreover, cholesterol oxidase has been found to selectively inhibit the function of caveolae (a special type of raft) (Okamoto *et al.*, 2000). Conditions of cholesterol oxidase treatment in 3A9 cells were first calibrated so that neither cell viability nor TCR surface expression was affected (not shown). The cholesterol oxidase treatment was found to strongly reduce the quantity of rafts detected in sucrose gradient (Figure 4A), and severely impaired the TCR-CD3-induced phosphorylation of CD3 $\zeta$ , ZAP-70 and LAT in the total cell lysate (Figure 4B). Of note, cholesterol oxidase alone did not induce these phosphorylation events (Figure 4B). Hence, these results strongly indicate that rafts are critically required in the initiation of TCR signaling.

#### **TCR-CD3 is concentrated in a subset of rafts**

Recent studies suggest that different raft populations may exist within the same cell membrane (Madore *et al.*, 1999; Roper *et al.*, 2000; Gomez-Mouton *et al.*, 2001). Therefore, we were interested in determining whether TCR is homogeneously distributed in T cell rafts. We have compared raft microdomains immunoprecipitated via TCR or Thy-1. To this end, raft membrane vesicles isolated from 3A9 cells were precipitated with either the CD3 $\epsilon$ - or Thy-1-specific mAb. Figure 5A (upper panels) shows that regardless of TCR stimulation by the HEL peptide, more CD3 chains were seen in the rafts immunoprecipitated with anti-CD3 than with anti-Thy-1. In stark contrast, a very low level of Thy-1 was found in the CD3-immunoprecipitated rafts compared with the Thy-1-immunoprecipitated ones. The distribution pattern of LAT in the immunoprecipitates was very similar to that of Thy-1, while that of Lck was somewhat intermediate: its reduction in the CD3-immunoprecipitated rafts relative to the Thy-1-immunoprecipitated rafts appeared to be less important than those of Thy-1 and LAT. [<sup>14</sup>C]cholesterol and [<sup>3</sup>H]phos-phatidylcholine labeling experiments (Figure 5B) indicated a similar cholesterol enrichment, relative to the unfractionated membrane fraction in the PNS, for both immunoprecipitates. However, there was probably at least 10-fold less of the membrane precipitated by anti-CD3 than anti-Thy-1 under our experimental conditions. These observations suggest that TCR-CD3 raft distribution is not homogenous and that a subset of rafts exhibit a particularly high TCR:Thy-1 ratio ('TCR rafts') than do others. The lower level of Thy-1 in the TCR rafts may well be apparent due to a lower membrane content in the CD3 precipitates. We next carried out sequential immunoprecipitation experiments. Figure 5C shows that although a pre-depletion of TCR-containing rafts did not significantly change the amount of Thy-1 that can be precipitated (upper panels), a pre-depletion of Thy-1-containing rafts quantitatively removed the TCR in raft preparations (lower panels). These findings support the idea that the TCR raft subset represents a very minor fraction of Thy-1-containing rafts.

TCR stimulation did not significantly modify the distribution pattern of all the molecules examined in the immunoprecipitates (the slight increase of Thy-1 and LAT in the CD3 isolates after TCR stimulation was not consistently observed). As expected, the CD3-precipitated rafts

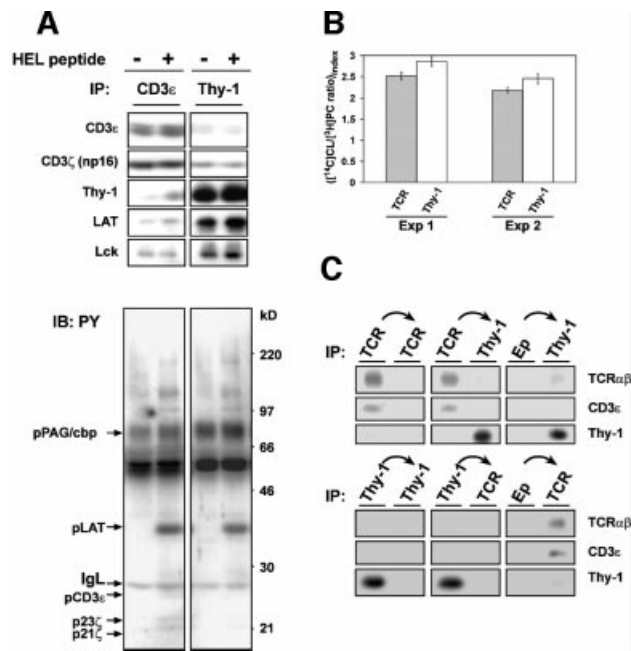


**Fig. 5.** (A) 3A9 cells were stimulated or not with the HEL peptide for 30 s at 37°C, as in Figure 3B. Isolated rafts were precipitated with 20  $\mu$ l of protein A–Eupergit beads pre-bound with the same amount (1  $\mu$ g) of anti-CD3 $\epsilon$  or anti-Thy-1 mAb. Immunoprecipitates were blotted with the indicated Abs. (B) 3A9 cells were labeled with [ $^{14}$ C]cholesterol and [ $^3$ H]cholinechloride as described in the Supplementary data. Isolated rafts were precipitated as in (A). [ $^{14}$ C]cholesterol and [ $^3$ H]phosphatidylcholine present in the total PNS membranes and the immunoprecipitates were determined as described in the Supplementary data. The index of [ $^{14}$ C]cholesterol to [ $^3$ H]phosphatidylcholine ratio for the immunoprecipitates was calculated by considering that for the corresponding total PNS membranes as 1 unit. Values are means  $\pm$  SE of the duplicates. Two individual experiments that are representative of four independent ones are shown. In experiment 1, the yields of [ $^{14}$ C]cholesterol are 6301  $\pm$  401 d.p.m. and 72 069  $\pm$  4730 d.p.m. for the CD3 and Thy-1 precipitates, respectively; while those of [ $^3$ H]phosphatidylcholine are 20 137  $\pm$  1985 d.p.m. and 202 511  $\pm$  5641 d.p.m. for the CD3 and Thy-1 precipitates, respectively. In experiment 2, the yields of [ $^{14}$ C]cholesterol are 4380  $\pm$  675 d.p.m. and 58 945  $\pm$  6667 d.p.m. for the CD3 and Thy-1 precipitates, respectively; while those of [ $^3$ H]phosphatidylcholine are 31 817  $\pm$  4048 d.p.m. and 379 795  $\pm$  25 434 d.p.m. for the CD3 and Thy-1 precipitates, respectively. (C) Isolated rafts were submitted to three rounds of precipitation with 20  $\mu$ l of protein A–Eupergit pre-bound without (Ep), or with 1  $\mu$ g anti-TCR $\beta$  mAb (upper panels) or 1  $\mu$ g anti-Thy-1 mAb (lower panels). The resulting supernatants were then precipitated with 20  $\mu$ l of protein A–Eupergit pre-bound with 1  $\mu$ g anti-TCR $\beta$  or anti-Thy-1 mAb. The precipitates were then blotted with the indicated Abs. In each series of precipitation, only results of the first and the last precipitation are shown.

contained more phospho-CD3 chains than the Thy-1-precipitated ones (Figure 5A, lower panel). To our surprise, a comparable level of phospho-LAT was found in the two immunisolates, which indicates that the LAT in the CD3-immunisolated rafts is extremely rich in its phospho isoform, considering the low LAT abundance in this compartment. These findings are in accordance with the fact that the earliest TCR signaling steps are activated in TCR rafts. To further investigate TCR signaling initiation in TCR rafts, 3A9 cells were stimulated with anti-CD3 $\epsilon$  mAb for 30 s and the isolated raft vesicles were then directly precipitated with TCR–CD3-bound activat-

ing mAb. Supplementary figure 4 indicates that these anti-CD3 mAbs precipitated a very similar raft subset as that seen in Figure 5A, which provides further evidence that it is within these TCR rafts that TCR is recognized by its ligand and activated. In this experiment, a large excess of anti-Thy-1, inefficient for CD3 isolation, was able to pull down higher amounts of phospho-LAT than was anti-CD3, suggesting that a significant fraction of the phospho-LAT obtained following TCR stimulation does not associate with TCR rafts. Collectively, these data reveal the existence of a TCR raft subset wherein the TCR initiates signaling pathways upon ligation. They also suggest the presence of raft populations that have either a very low level of TCR, or none at all ('non-TCR rafts'), which nonetheless participate actively in TCR signaling (see Discussion).

#### The CD4 co-receptor co-localizes with TCR in TCR rafts

The CD4 co-receptor plays an important role in potentiating TCR recognition in T helper cells (Janeway, 1992). It binds to class II MHC simultaneously with the TCR, or perhaps very shortly after TCR–pMHC engagement, and brings Lck to the engaged TCR (Janeway, 1992; Davis *et al.*, 1998). Experimental evidence suggests that CD4, despite the likely absence of direct interactions with TCR (Wang *et al.*, 2001), could be pre-organized at the vicinity of the TCR prior binding to MHC (Chuck *et al.*, 1990). CD4 has also been shown to partition into rafts (for a review see Harder, 2001). We have therefore examined the association of CD4 with the TCR raft subset in 3A9 T cells. Figure 6A shows that in non-stimulated cells, more CD4 was precipitated with anti-TCR than with anti-Thy-1 mAb, suggesting that CD4 is constitutively enriched in TCR rafts. Considering that much less membrane is likely to be found in the TCR precipitates, such an enrichment may in fact be a very high level. TCR stimulation did not change the CD4 partitioning in TCR rafts, at least in our stimulation conditions (30 s). Furthermore, we found that a TCR–CD4 'association' could be detected biochemically, but only in the raft compartment and only if raft integrity was preserved (Figure 6B). Together, these observations suggest that TCR rafts are involved in the pre-assembly of the CD4 co-receptor with TCR, a role of rafts so far unrecognized, which could be of particular importance in TCR signaling. Finally, the co-ligation of TCR–CD3 with CD4 resulted in a strong enhancement of the phosphorylation of CD3 $\zeta$  in TCR rafts (Figure 6C), which is consistent with the proposition that TCR triggers the signal initiation in these raft membrane microdomains.

#### TCR ligation triggers its early signaling pathways in the isolated TCR rafts

The existence of the TCR rafts prompted us to investigate whether the early TCR signaling pathways can be initiated in this raft subset in an autonomous fashion. To test this hypothesis, we examined protein tyrosine phosphorylation triggered by TCR–CD3 ligation in the TCR rafts isolated from unstimulated 3A9 T cells, in the presence of the exogenously added ATP. As depicted in Figure 7A, TCR–CD3 ligation induced the tyrosine phosphorylation of a series of proteins that displayed molecular weights ranging from 20 to 180 kDa. The 25 and 20–23 kDa Ptyr

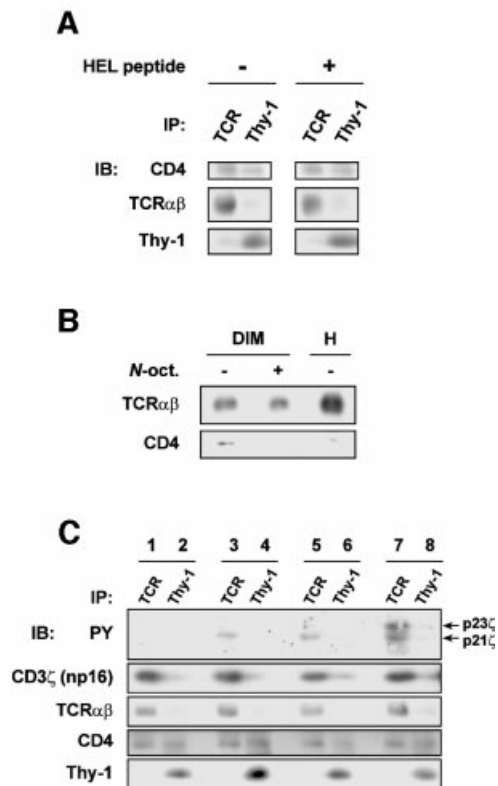


**Fig. 6.** (A) Rafts were isolated from 3A9 cells stimulated or not with the HEL peptide, and precipitated with 20  $\mu$ l of protein A–Eupergit pre-bound with 1  $\mu$ g anti-TCR $\beta$  or anti-Thy-1 mAb. The precipitates were blotted with the indicated mAbs. (B) Raft (DIM) and non-raft (H) fractions were prepared from unstimulated 3A9 cells. DIMs treated with or without 60 mM *N*-octylglucoside and the H fraction were then submitted to immunoprecipitation with anti-TCR $\beta$  mAb. The precipitates were blotted with the indicated mAbs. (C) 3A9 cells were mock stimulated (lanes 1 and 2) or stimulated for 30 s with either 10  $\mu$ g/ml of KT3 anti-CD3 $\epsilon$  mAb + 30  $\mu$ g/ml of rabbit anti-rat Ig (Fab')<sub>2</sub> (lanes 3 and 4), 20  $\mu$ g/ml of KT3 + 60  $\mu$ g/ml of rabbit anti-rat Ig (Fab')<sub>2</sub> (lanes 5 and 6) or 10  $\mu$ g/ml of KT3 + 10  $\mu$ g/ml of H129-19 anti-CD4 mAb + 60  $\mu$ g/ml of rabbit anti-rat Ig (Fab')<sub>2</sub> (lanes 7 and 8). Rafts were isolated and precipitated as in (A). The precipitates were blotted with the indicated mAbs. Note that neither KT3 nor H129-19 binds to protein A, and KT3 is less efficient in activating TCR–CD3 than 145-2C11.

proteins were identified as phospho-CD3 $\epsilon$  and phospho-CD3 $\zeta$ , respectively. Most of the phospho-CD3 $\zeta$  migrated at 23 kDa, which suggests some differences in the regulation of the CD3 $\zeta$  phosphorylation in isolated rafts relative to the intact cells, possibly by the protein tyrosine phosphatases (Germain, 2001). Nevertheless, we found that TCR–CD3 stimulation in the isolated rafts also triggered the tyrosine phosphorylation of ZAP-70 and LAT (Figure 7B). The signal corresponding to phospho-LAT following TCR–CD3 stimulation seemed to be less intense than that found in intact cells, presumably due to the absence of ZAP-70 recruitment from the cytosol and to a limited quantity of LAT in the TCR rafts. Moreover, we found that activation of TCR–CD3 in the isolated rafts was mediated by *src* kinases, since the treatment with PP2 completely abolished the phosphorylation of the CD3 chains (Figure 7C). Those results suggest that the activation of the TCR–CD3 complex in the isolated rafts triggered by receptor ligation is similar to that occurring in intact cells. Thus, the signaling molecule repertoire pre-

assembled in TCR rafts appears to be sufficient for TCR signal transduction initiation upon ligation.

## Discussion

In this study, we have shown that membrane microdomains, possessing the predicted characteristics of rafts, could be identified and isolated based on their resistance at 37°C to the polyoxyethylene detergent Brij 98. Analysis of the molecular organization of these microdomains has shed new light onto the involvement of rafts in signal transduction mediated by the TCR.

Our data further support the existence of rafts in cell membranes under physiological conditions. Besides T cells, we have also been able to isolate Brij 98 DIMs present at 37°C from a variety of other cell types (our unpublished results). Brij 98 DIMs, while isolated from mouse thymocytes, were visualized as membrane vesicles that exhibit a broad range of sizes with a mean vesicle diameter of  $67 \pm 39$  nm. In the membrane plane, the domains would be  $134 \pm 78$  nm in diameter, which is quite close to the raft size of  $\sim 50$  nm estimated by photonic force microscopy in living fibroblasts (Pralle *et al.*, 2000). However, it is not clear at present whether Brij 98 DIMs represent non-random assemblies of a limited number of elementary rafts. In any case, it is legitimate to think that these microdomains reflect a specific membrane organization, which is not induced by the detergent (see below). The efficient receptor-mediated signal transduction in the isolated microdomains also supports the notion that these membrane complexes closely correspond to a native structure. Our results also imply a significant stability of rafts at 37°C, which is in full agreement with the observation that rafts diffuse as a stable entity at the cell surface (Pralle *et al.*, 2000) that can persist for a strikingly long period of time (>20 min; J.K.Hörber, personal communication).

The biochemical characterization of membrane rafts is essential for their structural and functional studies. The new raft isolation method described here is a more advanced technique than the traditional cold Triton X-100-based one. The new method allowed us to specifically analyze only those rafts that are present at physiological temperature. This is of particular importance considering that chilling promotes formation of more of the lo membrane phase (Brown and London, 2000). On the other hand, Triton X-100 has been found to substantially solubilize lo phases, even at 4°C (Schroeder *et al.*, 1998; Brown and London, 2000), and failed to efficiently detect protein association to rafts of weak affinity (Janes *et al.*, 1999; Vidalain *et al.*, 2000). Finally, the detergent-resistant membrane domains isolated by cold Triton X-100 have a vesicle diameter generally between 0.5 and 1  $\mu$ m (Brown and London, 1998), which probably results from the coalescence of segregated raft units (Mayor and Maxfield, 1995; Madore *et al.*, 1999). In contrast, we have shown that during the new isolation procedure, raft microdomains from different cell membranes do not coalesce and raft subsets with different protein compositions from the same membrane could actually be isolated.

Although a number of studies have ascribed an essential role for rafts in the T cell activation, it has not been clearly

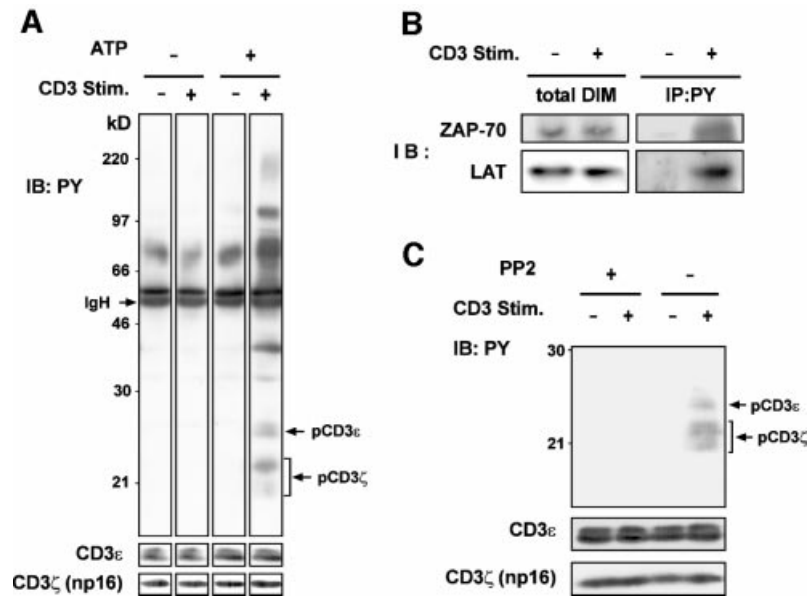


**Fig. 7.** (A) Rafts isolated from unstimulated 3A9 cells were diluted in the kinase buffer and incubated with or without 5  $\mu$ g/ml of anti-CD3 $\epsilon$  mAb and in the presence or not of 5  $\mu$ M ATP for 5 min at 37°C. Control experiments indicated a similar overall ATP loading in the stimulated and unstimulated raft vesicles (data not shown). The TCR raft subset was immunoprecipitated by anti-CD3 $\epsilon$  mAb as described in Materials and methods. The proteins were blotted with anti-PY mAb. The positions of the phospho-CD3 $\epsilon$  and phospho-CD3 $\zeta$  are indicated. The blot was then stripped and reprobed with anti-CD3 Abs. (B) Rafts isolated from unstimulated 3A9 cells were incubated with or without 5  $\mu$ g/ml of 145-2C11 in the presence of 5  $\mu$ M ATP, and then solubilized by *N*-octylglucoside at 4°C before precipitation with 4G10 anti-PY mAb and blotting with the indicated Abs. The total ZAP-70 and LAT content in DIMs are also shown. (C) Rafts isolated from 3A9 cells were pre-treated with or without 10 mM PP2 for 5 min at 37°C before being submitted to TCR or mock stimulation in the presence of 5  $\mu$ M ATP. The phosphorylation of CD3 chains in the TCR raft subset was analyzed by blotting. The blot was then stripped and reprobed with anti-CD3 Abs.

established whether rafts are involved in the earliest steps of the TCR signaling. We have provided the answer in the present study by showing that the TCR signal initiation machinery is comprised of the TCR-CD3 complex, Lck and ZAP-70 kinases, and the CD4 co-receptor is pre-assembled and activated upon receptor ligation in a subset of rafts. A constitutive (and *src* kinase activity-independent) association of TCR with Brij 98 DIMs also eliminates the suspicion that TCR-raft association is an *in vitro* artifact arising as a consequence of trapping ligand-engaged TCR oligomers into DIMs following membrane solubilization. The finding that raft disruption following cholesterol oxidase blocks TCR-CD3 activation further strengthens our proposal that rafts are required for the initiation of TCR signaling. Finally, the fact that TCR ligation triggers early signaling pathways in isolated TCR rafts indicates that this raft subset is fully competent for TCR signal initiation. Our model of TCR signal initiation within rafts is consistent with the observations that (membrane-associated) Lck acylation mutants are ineffective for TCR-CD3 phosphorylation (Kabouridis *et al.*, 1997; Kosugi *et al.*, 2001).

Using cold Triton X-100 or Brij 58, we and others previously found that stimulation of TCR caused more of the receptors to associate with detergent resistant domains (Montixi *et al.*, 1998; Xavier *et al.*, 1998). It was therefore proposed that TCR is recruited to rafts upon ligation. This result, in apparent discrepancy with the present work, could be explained by the following observation. If the Brij 98 DIMs isolated from non-stimulated and TCR-stimulated cells were subsequently treated with Triton

X-100 (or Brij 58; data not shown) at 4°C, a differential solubilization was observed (Supplementary figure 5). Indeed, a more marked diminution of raft-associated TCR-CD3 was found in non-stimulated cells than in TCR-stimulated cells. These findings suggest that the previously observed TCR recruitment probably reflects an enhanced resistance of TCR association with rafts in Triton X-100 (and Brij 58) upon engagement by the ligand, rather than a receptor translocation to rafts.

The presence of raft subsets with different protein compositions in the same membrane is rather expected when considering that rafts are very small and that specific interactions exist between different raft-associated proteins (Simons and Toomre, 2000). Our findings on the TCR rafts are consistent with this notion. Further investigations will be required to characterize this raft population in more detail, especially in terms of lipid composition. Nevertheless, we think that our data have uncovered an important ability of raft microdomains to pre-assemble signal transduction units. Within these assembled units, dynamic (and probably often weak) interactions probably take place. This is exemplified by the co-localization of TCR and CD4 in the TCR rafts. During recognition of pMHC by T cells, CD4 is believed to bind to the same pMHC molecule as the TCR (for a review see Janeway, 1992), which contributes to the recruitment of the Lck to the engaged TCR-CD3 complex and 'boosts' TCR recognition (Janeway, 1992; Davis *et al.*, 1998; Krummel *et al.*, 2000). Nonetheless, the molecular mechanism underlying the dual TCR and CD4 binding has been puzzling. Owing to the off-rate of the TCR-pMHC



interaction (for a review see Davis *et al.*, 1998), CD4 would have to bind to the same pMHC complex quasi-simultaneously to the TCR. This is, however, in apparent contradiction with the fact that CD4 binding to class II MHC is of extremely low affinity (Xiong *et al.*, 2001) and there seem to be no direct interactions between TCR and CD4 (Wang *et al.*, 2001). Thus, a confined CD4 localization in TCR rafts would increase its binding with the TCR-engaged MHC molecule, by favoring rebound over diffusion away, resulting at the same time in a very dynamic CD4–MHC interaction. Our model is consistent with the observation that a fraction of CD4 molecules is found in the vicinity of the TCR prior binding to MHC (Chuck *et al.*, 1990). Such a dynamic CD4–MHC interaction could be important for the CD4–Lck complex to associate in a discriminative manner with the engaged TCR and amplify the activation signals only above a certain threshold of TCR engagement (Davis *et al.*, 1998). It will be particularly interesting to determine whether rafts also contribute to the pre-association of TCR with the CD8 co-receptor (Arcaro *et al.*, 2001).

Our results also suggest that the signals initiated in TCR rafts are rapidly propagated into non-TCR rafts. Indeed, a significant proportion of phospho-LAT is localized in these membrane domains upon TCR stimulation (Figure 6B). A challenge for the future will be to understand how different raft subsets communicate with each other during TCR signaling. One possibility is raft coalescence (see below). In addition, signaling molecules could shuttle between different raft subsets. In this context, we observed that although LAT molecules are most strongly phosphorylated in TCR rafts, the majority of them are located in non-TCR rafts. Of interest, Wilson *et al.* have recently proposed that activated mast cells propagate signals from primary domains organized around the FcεRI and from secondary domains, including one organized around LAT (Wilson *et al.*, 2000, 2001).

We would like to emphasize that in this study we have focused on the very early steps of the TCR-dependent signaling, which take place within seconds of receptor engagement. However, following the initiation phases, signaling should be sustained to promote full T cell activation (Viola *et al.*, 1999). One mechanism involved in the signal sustaining is probably raft coalescence (Simons and Toomre, 2000), which can be promoted, for instance, by linker molecules, and be homotypic or heterotypic in nature. Interestingly, microscopy analysis in living cells has revealed that the initial TCR response coincides with the appearance of small, dispersed clusters of CD3ζ and CD4 at the T cell–antigen presenting cell interface (Krummel *et al.*, 2000). These clusters eventually coalesce to form a larger cluster at the central zone of the immunological synapse, where the micrometer-sized raft patches are found to be co-localized upon activation of an intracellular pathway involving Vav1, Rac and actin cytoskeleton reorganization (Villalba *et al.*, 2001).

In summary, our findings reported here strongly support the notion that rafts represent molecular sorting machines (Simons and Ikonen, 1997; Brown and London, 1998) capable of organizing signal transduction pathways within specific areas of the membrane,

both prior to and following receptor engagement by ligand, to expedite selective and efficient activation of signaling cascades upon stimulation.

## Materials and methods

### Cells and reagents

See Supplementary data.

### PNS and membrane preparation

Cells were gently sonicated (five 5-s bursts, 5 W; Vibracell, Bioblock Scientific) in 1 ml of ice-cold buffer A (25 mM HEPES, 150 mM NaCl, 1 mM EGTA, 5 mM NaVO<sub>4</sub>, 10 mM NaP–P and 10 mM NaF, 1 μg/ml leupeptin, 1 μg/ml pepstatin, 2 μg/ml chymostatin and 5 μg/ml α<sub>2</sub> macroglobulin). The PNS was obtained after centrifugation at 800 g at 4°C for 10 min. The membrane fraction was obtained by pelleting the PNS at 100 000 g for 1 h at 4°C.

### DIM isolation

PNS from (2 × 10<sup>8</sup>) mouse thymocytes or nylon wool-purified splenic T lymphocytes, or from (3 × 10<sup>7</sup>) 3A9 or AKR1 mouse T cells was pre-incubated for 4 min at 37°C. Brij 98 (Sigma Chemical Co.) was then added to a final concentration of 1%. After 5 min of solubilization at 37°C, the PNS (1 ml) was diluted with 2 ml 37°C pre-warmed buffer A containing 2 M sucrose (final sucrose concentration 1.33 M; final Brij 98 concentration 0.33%) and chilled down on ice (55 min) before being placed at the bottom of a step sucrose gradient (0.9–0.8–0.75–0.7–0.6–0.5–0.4–0.2 M sucrose, 1 ml each) in buffer A. Gradients were centrifuged at 38 000 r.p.m. for 16 h in a SW41 rotor (Beckman Instruments Inc.) at 4°C. One milliliter fractions were harvested from the top, except for the last one (no. 9), which contains 3 ml. Unless specified, DIM fraction is pooled fractions 2–5 and H fraction is pooled fractions 8 and 9.

### TCR–CD3 stimulation by pMHC

LK35.2 cells pulsed overnight with 3 μM HEL 48–63 peptide were pre-fixed with 0.8% paraformaldehyde in phosphate-buffered saline for 30 min at 4°C, followed by incubation with 0.2 M lysine for 10 min. These treatments fully preserve the capacity of LK35.2 to activate TCR signaling pathways while preventing their rafts from floating in the sucrose density gradient. For TCR stimulation, 3A9 cells were put in contact with LK35.2 cells by centrifugation for 10 s at 400 g and incubated for 30 s at 37°C. One milliliter of ice-cold buffer A was immediately added to cell pellets, followed by sonication.

### TCR–CD3 stimulation in the isolated DIMs

DIMs from 1 × 10<sup>7</sup> 3A9 cells were concentrated before being resuspended in 200 μl of the kinase buffer (20 mM HEPES, 150 mM NaCl, 5 mM MgCl<sub>2</sub>, 5 mM MnCl<sub>2</sub>, 1 mM NaVO<sub>4</sub>) at room temperature. DIMs were then incubated with 1 μg of anti-CD3ε mAb 145-2C11 (5 μg/ml) in the presence of 5 μM of ATP for 5 min at 37°C. The phosphorylation reaction was stopped by addition of 1 ml of ice-cold buffer B (20 mM HEPES, 150 mM NaCl, 20 mM EDTA, 5 mM NaVO<sub>4</sub> and protease inhibitors). Unless specified, 10 μl of protein A-immobilized Eupergit beads, or 10 μl of protein A-immobilized Eupergit beads plus 1 μg of 145-2C11 mAb was used to immunoprecipitate the TCR DIM subset from the TCR–CD3 stimulated cells and the controls, respectively.

### Supplementary data

Supplementary data for this paper are available at *The EMBO Journal* Online.

## Acknowledgements

We wish to thank J.K.Hörber for permitting us to mention unpublished data; P.Chavrier, V.Horejsi, B.Malissen and J.Nunez for providing us with antibodies; L.Leserman and R.Hyman for cell lines; S.Meresse, S.Granjeaud and O.Chambenoit for technical advice; and P.Fourquet for peptide synthesis. We thank J.Ewbank, P.Golstein, A.-O.Hueber, S.Kerrige, A.C.Lellouch, B.Malissen, D.Marguet, P.Naquet, P.Pierre, Q.Sattentau, A.-M.Schmitt-Verhulst, E.Van Obberghen-Schilling and C.Zou for helpful discussions and critical reading of the manuscript. This work was supported by institutional funds from Institut National de la Santé et de la Recherche Médicale (INSERM), the Centre National

de la Recherche Scientifique (CNRS), and by grants from Association pour la Recherche contre le Cancer (ARC) and Ligue Nationale Française Contre le Cancer (LNFFCC).

## References

- Arcaro, A. et al. (2001) CD8 $\beta$  endows CD8 with efficient coreceptor function by coupling T cell receptor/CD3 to raft-associated CD8/p56(lck) complexes. *J. Exp. Med.*, **194**, 1485–1495.
- Brown, D.A. and London, E. (1998) Functions of lipid rafts in biological membranes. *Annu. Rev. Cell. Dev. Biol.*, **14**, 111–136.
- Brown, D.A. and London, E. (2000) Structure and function of sphingolipid- and cholesterol-rich membrane rafts. *J. Biol. Chem.*, **275**, 17221–17224.
- Chuck, R.S., Cantor, C.R. and Tse, D.B. (1990) CD4–T-cell antigen receptor complexes on human leukemia T cells. *Proc. Natl Acad. Sci. USA*, **87**, 5021–5025.
- Davis, M.M., Boniface, J.J., Reich, Z., Lyons, D., Hampl, J., Arden, B. and Chien, Y. (1998) Ligand recognition by  $\alpha\beta$  T cell receptors. *Annu. Rev. Immunol.*, **16**, 523–544.
- Germain, R.N. (2001) The T-cell receptor for antigen: Signaling and ligand discrimination. *J. Biol. Chem.*, **276**, 35223–35226.
- Gomez-Mouton, C. et al. (2001) Segregation of leading-edge and uropod components into specific lipid rafts during T cell polarization. *Proc. Natl Acad. Sci. USA*, **98**, 9642–9647.
- Harder, T. (2001) Raft membrane domains and immunoreceptor functions. *Adv. Immunol.*, **77**, 45–92.
- Janes, P.W., Ley, S.C. and Magee, A.I. (1999) Aggregation of lipid rafts accompanies signaling via the T cell antigen receptor. *J. Cell Biol.*, **147**, 447–461.
- Janeway, C.A. (1992) The T cell receptor as a multicomponent signalling machine: CD4/CD8 coreceptors and CD45 in T cell activation. *Annu. Rev. Immunol.*, **10**, 645–674.
- Kabouridis, P.S., Magee, A.I. and Ley, S.C. (1997) S-acylation of LCK protein tyrosine kinase is essential for its signalling function in T lymphocytes. *EMBO J.*, **16**, 4983–4998.
- Kabouridis, P.S., Janzen, J., Magee, A.I. and Ley, S.C. (2000) Cholesterol depletion disrupts lipid rafts and modulates the activity of multiple signaling pathways in T lymphocytes. *Eur. J. Immunol.*, **30**, 954–963.
- Kosugi, A., Hayashi, F., Liddicoat, D.R., Yasuda, K., Saitoh, S. and Hamaoka, T. (2001) A pivotal role of cysteine 3 of Lck tyrosine kinase for localization to glycolipid-enriched microdomains and T cell activation. *Immunol. Lett.*, **76**, 133–138.
- Krummel, M.F., Sjaastad, M.D., Wulfig, C. and Davis, M.M. (2000) Differential clustering of CD4 and CD3 $\zeta$  during T cell recognition. *Science*, **289**, 1349–1352.
- Langlet, C., Bernard, A.M., Drevot, P. and He, H.T. (2000) Membrane rafts and signaling by the multichain immune recognition receptors. *Curr. Opin. Immunol.*, **12**, 250–255.
- Liu, H., Rhodes, M., Wiest, D.L. and Vignali, D.A. (2000) On the dynamics of TCR:CD3 complex cell surface expression and downmodulation. *Immunity*, **13**, 665–675.
- Madore, N., Smith, K.L., Graham, C.H., Jen, A., Brady, K., Hall, S. and Morris, R. (1999) Functionally different GPI proteins are organized in different domains on the neuronal surface. *EMBO J.*, **18**, 6917–6926.
- Mayor, S. and Maxfield, F.R. (1995) Insolubility and redistribution of GPI-anchored proteins at the cell surface after detergent treatment. *Mol. Biol. Cell*, **6**, 929–944.
- Melkonian, K.A., Ostermeyer, A.G., Chen, J.Z., Roth, M.G. and Brown, D.A. (1999) Role of lipid modifications in targeting proteins to detergent-resistant membrane rafts. Many raft proteins are acylated, while few are prenylated. *J. Biol. Chem.*, **274**, 3910–3917.
- Montixi, C., Langlet, C., Bernard, A.M., Thimonier, J., Dubois, C., Wurbel, M.A., Chauvin, J.P., Pierres, M. and He, H.-T. (1998) Engagement of T cell receptor triggers its recruitment to low-density detergent-insoluble membrane domains. *EMBO J.*, **17**, 5334–5348.
- Moran, M. and Miceli, M.C. (1998) Engagement of GPI-linked CD48 contributes to TCR signals and cytoskeletal reorganization: a role for lipid rafts in T cell activation. *Immunity*, **9**, 787–796.
- Okamoto, Y., Ninomiya, H., Miwa, S. and Masaki, T. (2000) Cholesterol oxidation switches the internalization pathway of endothelin receptor type A from caveolae to clathrin-coated pits in Chinese hamster ovary cells. *J. Biol. Chem.*, **275**, 6439–6446.
- Pralle, A., Keller, P., Florin, E.L., Simons, K. and Horber, J.K. (2000) Sphingolipid-cholesterol rafts diffuse as small entities in the plasma membrane of mammalian cells. *J. Cell Biol.*, **148**, 997–1008.
- Roper, K., Corbeil, D. and Huttner, W.B. (2000) Retention of prominin in microvilli reveals distinct cholesterol-based lipid micro-domains in the apical plasma membrane. *Nature Cell Biol.*, **2**, 582–592.
- Schroeder, R.J., Ahmed, S.N., Zhu, Y., London, E. and Brown, D.A. (1998) Cholesterol and sphingolipid enhance the Triton X-100 insolubility of glycosylphosphatidylinositol-anchored proteins by promoting the formation of detergent-insoluble ordered membrane domains. *J. Biol. Chem.*, **273**, 1150–1157.
- Simons, K. and Ikonen, E. (1997) Functional rafts in cell membranes. *Nature*, **387**, 569–572.
- Simons, K. and Toomre, D. (2000) Lipid rafts and signal transduction. *Nature Rev. Mol. Cell Biol.*, **1**, 31–39.
- van Oers, N.S., Tohlen, B., Malissen, B., Moomaw, C.R., Afendis, S. and Slaughter, C.A. (2000) The 21- and 23-kD forms of TCR zeta are generated by specific ITAM phosphorylations. *Nature Immunol.*, **1**, 322–328.
- Vidalain, P.O., Azocar, O., Servet-Delprat, C., Rabourdin-Combe, C., Gerlier, D. and Manie, S. (2000) CD40 signaling in human dendritic cells is initiated within membrane rafts. *EMBO J.*, **19**, 3304–3313.
- Villalba, M., Bi, K., Rodriguez, F., Tanaka, Y., Schoenberger, S. and Altman, A. (2001) Vav1/Rac-dependent actin cytoskeleton reorganization is required for lipid raft clustering in T cells. *J. Cell Biol.*, **155**, 331–338.
- Viola, A., Schroeder, S., Sakakibara, Y. and Lanzavecchia, A. (1999) T lymphocyte costimulation mediated by reorganization of membrane microdomains. *Science*, **283**, 680–682.
- Wang, J.H., Meijers, R., Xiong, Y., Liu, J.H., Sakihama, T., Zhang, R., Joachimiak, A. and Reinherz, E.L. (2001) Crystal structure of the human CD4 N-terminal two-domain fragment complexed to a class II MHC molecule. *Proc. Natl Acad. Sci. USA*, **98**, 10799–10804.
- Weiss, A. and Littman, D.R. (1994) Signal transduction by lymphocyte antigen receptors. *Cell*, **76**, 263–274.
- Wilson, B.S., Pfeiffer, J.R. and Oliver, J.M. (2000) Observing Fc $\epsilon$ RI signaling from the inside of the mast cell membrane. *J. Cell Biol.*, **149**, 1131–1142.
- Wilson, B.S., Pfeiffer, J.R., Surviladze, Z., Gaudet, E.A. and Oliver, J.M. (2001) High resolution mapping of mast cell membranes reveals primary and secondary domains of Fc $\epsilon$ RI and LAT. *J. Cell Biol.*, **154**, 645–658.
- Xavier, R., Brennan, T., Li, Q., McCormack, C. and Seed, B. (1998) Membrane compartmentation is required for efficient T cell activation. *Immunity*, **8**, 723–732.
- Xiong, Y., Kern, P., Chang, H. and Reinherz, E. (2001) T cell receptor binding to a pMHCII ligand is kinetically distinct from and independent of CD4. *J. Biol. Chem.*, **276**, 5659–5667.
- Xu, X. and London, E. (2000) The effect of sterol structure on membrane lipid domains reveals how cholesterol can induce lipid domain formation. *Biochemistry*, **39**, 843–849.
- Zhang, W. and Samelson, L.E. (2000) The role of membrane-associated adaptors in T cell receptor signalling. *Semin. Immunol.*, **12**, 35–41.
- Zhang, W., Tribble, R.P. and Samelson, L.E. (1998) LAT palmitoylation: its essential role in membrane microdomain targeting and tyrosine phosphorylation during T cell activation. *Immunity*, **9**, 239–246.

Received November 12, 2001; revised January 17, 2002;  
accepted February 21, 2002